Journal of Plant Growth Regulation
https://doi.org/10.1007/s00344-024-11564-9

Effect of Fumonisin B_1 on Transcriptional Profiles and Biochemical Signatures in Resistant and Susceptible Maize Shoots

Alessandra Lanubile[1] · Diana Bellin[2] · Letizia Ottaviani[1] · Mehrdad Jaberi[2] · Adriano Marocco[1] · Giuseppina Mulè[3] · Costantino Paciolla[4]

Received: 31 July 2023 / Accepted: 11 November 2024

Abstract

Fumonisin B_1 (FB_1) is the most harmful toxin, due to its incidence and high concentrations in maize, along with its toxicity to humans and animals. To investigate possible mechanisms of FB_1 phytotoxicity, an RNA-Sequencing based transcriptome analysis was carried out at 3 h after FB_1 treatment in the shoots of the CO433 maize line resistant to *Fusarium verticillioides*. One thousand four hundred and fifty-nine differentially expressed genes were identified, 13.9% of them playing a role in defense and cell rescue functional classes. The study of the transcriptional changes was extended to the CO389 genotype susceptible to *F. verticillioides* at 3 and 48 h after exposure to FB_1 for a subset of thirteen genes involved in the antioxidant metabolism, mycotoxin detoxification, cell death regulation, hormone signaling, and ubiquitination. Moreover, antioxidant enzymes and compounds were monitored in the same plant material. Defense responses appeared promptly activated in the shoots of the resistant genotype; particularly, at 3 h, the accumulation of most transcripts and enzymes protecting from oxidative stress and involved in the toxicity response processes as well as the ascorbate content were enhanced, underlining an earlier and higher attitude in this background to counteract the phytotoxic action of FB_1. In contrast, in the susceptible line, the expression of the majority of genes along with catalase, phenolics and ascorbate levels increased at later treatment time, conferring a lower readiness in response to the mycotoxin. This work provides useful sources of markers for the development of successful disease management strategies in maize.

Keywords Fumonisin B_1 · *Zea mays* · RNA-sequencing · Phytotoxicity · Antioxidant defense · Programmed cell death

Introduction

Maize (*Zea mays* L.) is a key crop for food, feed, and industrial applications. It showed the highest production in 2021 with more than 1.2 billion tons harvested and the fastest growth since 2000 Food and Agriculture Organization of the United Nations (2021). Across all its cultivation range, maize is highly exposed to significant constraints due to the presence of pathogens limiting grain yield and quality. Fungal diseases may affect maize cultivation, and the severity of infection is largely dependent on environmental conditions, the choice of cultural practice and the susceptibility of varieties used for breeding (Lanubile et al. 2014; Logrieco et al. 2021).

Fusarium spp. are amongst the most prominent maize pathogens and can infect plants at different development stages causing several pathologies such as seedling blights, ear rots, stalk rots, and root rots (Baldwin et al. 2014; Yates et al. 2011). During infection, *Fusarium* spp. can release

Handling Editor: Paloma Sanchez.

✉ Alessandra Lanubile
alessandra.lanubile@unicatt.it

[1] Department of Sustainable Crop Production, Università Cattolica del Sacro Cuore, Via Emilia Parmense 84, 29122 Piacenza, Italy

[2] Department of Biotechnology, University of Verona, Strada Le Grazie, 15, 37134 Verona, Italy

[3] Institute of Sciences of Food Production, National Research Council of Italy (CNR), Via Amendola 122/O, 70126 Bari, Italy

[4] Department of Biosciences, Biotechnology and Environment, Università Degli Studi Di Bari Aldo Moro, Via E. Orabona 4, 70125 Bari, Italy

Published online: 29 November 2024

various mycotoxins that represent important pathogenicity and virulence factors (Logrieco et al. 2021; Munkvold et al. 2021). One of these harmful mycotoxins is fumonisin B_1 (FB_1), which is the most toxic and prevalent among other fumonisins, recorded as a potential human carcinogen (group 2B) by the International Agency for Research on Cancer (1993). Moreover, its toxicity was ascertained in animals, causing diseases such equine leukoencephalomalacia, porcine pulmonary edema and hepatic cancer, and in plants, determining seedling length and dry mass reduction, chlorosis, necrosis, and programmed cell death (PCD) (Ismaiel and Papenbrock 2015; Renaud et al. 2021).

Fumonisin B1 (FB_1) is the structural analogue of the sphingoid bases sphinganine and sphingosine and inhibits metabolism of sphingolipids, the major structural components of plasma membrane, by the suppression of ceramide synthase activity (Wang et al. 2016; Zhao et al. 2022). Perturbations in the sphingolipid pathway and PCD in plants are strongly associated (Zeng et al. 2020). Long-chain bases (LCBs) serve as building block of sphingolipids and act as second messengers. It was observed that FB_1 treatment leads to an imbalance between free LCBs and ceramides that in turn cause PCD in a hormone-dependent manner (Asai et al. 2000; Nishimura et al. 2003; Shi et al. 2007). The overexpression of a sphingoid LCB kinase (*LCBK1*) in *Arabidopsis* induced plant resistance to FB_1 exposure, conversely its knockdown conferred hypersensitivity to the mycotoxin (Yanagawa et al. 2017). Moreover, supplying plants with the sphingoid bases dihydrosphingosine, phytosphingosine, and sphingosine efficiently triggered reactive oxygen intermediate production and cell death (Shi et al. 2007).

During plant-pathogen/elicitor interactions, the production of reactive oxygen species (ROS) is rapidly induced (Iqbal et al. 2021; Xing et al. 2013; Ye et al. 2021). ROS (e.g., H_2O_2, $O_2^{\cdot-}$, and $OH^{\cdot}$) and nitric oxide generation can initiate the hypersensitive response (HR), a form of PCD at the infection site, which results in a rapid and localized cell death restraining pathogen spread (Iqbal et al. 2021). In addition, protein and chloroplast oxidation, lipid peroxidation, cell and DNA damage can be caused by ROS production (Noctor et al. 2018). ROS surplus is regulated by the expression and activity of several antioxidant enzymes, including superoxide dismutase (SOD), catalase (CAT), ascorbate peroxidase (APX), and peroxidase (POD) (Poór et al. 2017). Moreover, plants have developed non-enzymatic defense antioxidants such as ascorbate (ASC), dehydroascorbate (DHA), glutathione (GSH) and glutathione oxidized (GSSH) (Foyer and Noctor 2009). Similarly, as in plant-pathogen interaction, a significant induction of superoxide and H_2O_2 was found under FB_1 stress in *Arabidopsis* leaves (Xing et al. 2013). In parallel, pre-treatments with CAT and ASC led to a drastic reduction of FB_1-induced ROS burst and salicylic acid levels (Xing et al. 2013). Analogous results were reported by Lanubile et al. (2022), where an even higher accumulation of H_2O_2 and superoxide, as well as GSH, was measured in cell cultures of the same plant species 48 h after FB_1 exposure. Moreover, a plethora of oxidative stress biomarkers as electrolyte leakage, H_2O_2, SOD, POD and thiobarbituric acids was assayed in resistant and susceptible maize seedlings irrigated with FB_1 (1 and 20 µg mL^{-1}) and sampled up to 21 days after planting (Otaiza-González et al. 2022). Plant redox status was perturbated mainly in roots at both mycotoxin concentrations, though the resistant plants showed a rapid induction of cell death and major stress at late treatment time indicative of a more efficient FB_1 phytotoxicity control strategy (Otaiza-González et al. 2022).

In the present study, an extensive view of the impact of FB_1 was investigated in resistant (CO433) and susceptible (CO389) to *Fusarium verticillioides* maize shoots at 3 and 48 h after treatment. RNA-Sequencing (RNA-Seq), real-time reverse transcription-quantitative PCR (RT-qPCR) analysis and enzymatic and compound measurements were combined to identify genes and antioxidant clues correlated with the phytotoxicity elicited by FB_1.

Materials and Methods

Plant Material and Fumonisin B_1 Treatment

Two maize genotypes with contrasting phenotypes for resistance to Fusarium ear rot were used in this study: the resistant line CO433 and the susceptible line CO389, as previously reported (Maschietto et al. 2016). Seeds were obtained from the Eastern Cereal and Oilseed Research Centre, Agriculture and Agri-Food Canada (Ottawa, Canada) and were maintained by sibbing at the Department of Sustainable Crop Production, Università Cattolica del Sacro Cuore, Piacenza, Italy.

Seeds of the two lines were planted in pots (40 cm diameter, 35 cm height) and plants of each line were grown in an environmentally controlled greenhouse with day- and night-time conditions of 28 °C and 20 °C temperatures, respectively, and a light regime of 16 h using lamps at 500 µmol m^{-2} s^{-1} (Master TLD 58 W/830, Royal Philips Electronics, Eindhoven, The Netherlands) as described in Lanubile et al. (2015). At the three-leaf stage, 40 sterile shoots of both lines were spiked by HPLC syringe injection with fumonisin B_1 (FB_1) (AppliChem, Germany), dissolved in Phosphate Buffered Saline (PBS) $pH = 7.4$ at the final concentration of 1 mg mL^{-1}, in the part of the stem between the collar and the insertion of the first leaf. In parallel, control shoots were inoculated with PBS without FB_1. Shoots were collected at 3 and 48 h after FB_1 and buffer treatment and analyzed. Four pools of shoots for the 3 and

48 h time-points were prepared, where each pool derived from the mixing of 10 plants of FB_1 and buffer inoculated CO433 and CO389 lines.

RNA-Seq analysis was conducted only on shoots of the CO433 genotype collected at 3 h after FB_1 and buffer treatment considering three biological replicates. To assess whether FB_1 treatment, by mimicking an HR response, caused a premature modulation of cell death responsive genes and a high level of oxidative stress, a very early time-point (3 h) after fumonisin elicitation was considered for the RNA-Seq experiments. Indeed, plants hypersensitive response by an incompatible pathogen interaction is characterized by an early oxidative and nitrosative burst. Moreover, maize shoot tissues were selected based on the results of a previous work by Desjardins et al. (1995), where the inoculation of a similar concentration of fumonisin resulted in decreased shoot emergence and seedling height compared with treatment without the mycotoxin.

Real-time reverse transcription-quantitative PCR (RT-qPCR) and enzymatic and other parameters analysis were performed on shoots of both genotypes at 3 and 48 h after FB_1 or buffer treatment. RT-qPCR experiments refer to three independent biological replicates as for RNA-Seq analysis, whereas biochemical experiments refer to four independent biological replicates.

RNA Isolation and Library Preparation

The collected shoots were ground in liquid nitrogen with a pestle and mortar and total RNA isolations were performed according to Lanubile et al. (2013) using TRIzol™ protocol (ThermoFisher SCIENTIFIC, Waltham, MA, USA). RNA was then purified with the RNA Clean up protocol (Qiagen, Valencia, CA, USA), according to the manufacturer's instructions. The extracted RNA was quantified using a fluorometric assay (Qubit, Thermo Fisher Scientific Inc. Waltham, MA, USA) and the integrity was checked using gel electrophoresis. Furthermore, total RNA samples were assessed for quality using an RNA 6000 Nano Kit (Agilent, Wokingham, UK) and 2.5-µg were utilized for the preparation of a non-directional Illumina RNA-Seq library using the TruSeq RNA Sample Prep Kit v2 (Illumina Inc., San Diego, CA, USA). The quality of the library was checked with a High Sensitivity DNA Kit (Agilent). Libraries were sequenced with an Illumina HiSeq 1000 sequencer (Illumina) and 100-bp paired-end sequences were generated. Raw sequences are available in the National Center for Biotechnology Information (NCBI) Sequence Read Archive (SRA) under accession number PRJNA1190998.

Bioinformatic Analysis

Raw and processed sequence data were assessed using FastQC v0.11.9 (https://www.bioinformatics.babraham.ac.uk/projects/fastqc, February 2024). TrimGalore v0.6.7 (https://github.com/FelixKrueger/TrimGalore, February 2024) and Cutadapt v3.4 (Martin 2011) were used for adapter and quality trimming for paired-end data with Phred quality score > 20 and minimum read length of 35 bp. Processed reads were aligned to the maize Zm-B73-REFERENCE-NAM-5.0 downloaded from Ensembl Plants Release 58 using STAR v2.7.9a (Dobin et al. 2013) in two-pass mode and transcript abundances were quantified using Salmon v1.5.2 (Patro et al. 2017). SAMtools v1.15.1 (Li et al. 2009) was used for sorting and indexing alignments. Data was processed using nf-core/rnaseq v3.14.0 (Patel et al. 2024) executed with Nextflow v23.05.0-edge (Di Tommaso et al. 2017). Quantification and statistical inference of systematic changes were investigated using DESeq2 v1.38.0 (Love et al. 2014). Differentially expressed genes (DEGs) were selected with adjusted p-value threshold of 0.05 and selecting genes with $Log2FC \geq 0.5$ or $Log2FC \leq -0.5$. The procedure of p-value adjustment for multiple testing was according to Benjamini and Hochberg (1995) as implemented in DESEq2 package.

Sequences of DEGs were compared with NCBI non redundant (NR) database with a Blast E-value of 10^{-3} and were functionally annotated using Blast2GO (Götz et al. 2008) assigning a GO term and a metabolic pathway in the Kyoto Encyclopaedia of Genes and Genomes (KEGG) to the query sequences. Sequences were classified into 13 functional categories (Cell component; Cell wall; Electron/Energy; Metabolic process; Miscellanea; Photosynthesis; Proteolysis; Response to stress; Resistance; Secondary metabolism; Signal transduction; Transport; Unknown function) based on GO annotation.

Real-Time RT-qPCR Gene Expression Analysis

As already mentioned above, RT-qPCR experiments were performed on shoots collected at 3 and 48 h after FB_1 and buffer treatment for the genotypes CO433 and CO389 using the FluoCycleTM II SYBR Green master mix (EuroClone S.p.a., Milan, Italy) and the CFX-96 device (Bio-Rad, Hercules, CA, USA). One µg of total RNA was taken for cDNA synthesis using the High Capacity cDNA Reverse Transcription Kit (Thermo Fisher Scientific). For real-time RT-qPCR, 20 ng of single strand cDNA determined by fluorometric assay (Qubit, Thermo Fisher Scientific). RT-qPCR was performed under the following conditions: 95 °C for 3 min and 40 cycles at 95 °C for 15 s, specific annealing temperatures for 30 s, followed by a melting curve analysis. For each of the three biological replicates, three technical

replicates were employed for each FB_1 treated sample and buffer treated controls. When possible, gene-specific primers were designed within consecutive exons, separated by an intron, using Primer3 software and their sequences are listed in Supplementary Table 1. Relative quantification was normalized to the housekeeping control gene (*β-actin*) and fold change (FC) values in gene expression were calculated using the $2^{-\Delta\Delta Ct}$ method (Schimittgen and Livak 2008) and calibrated on the buffer treated control.

Enzymatic Activity Determination

Fumonisin B_1 and buffer treated shoots of CO433 and CO389 genotypes were ground with a pestle and mortar at 4 °C in 50 mM Tris–HCl pH 7.8 containing 0.3 mM mannitol, 1 mM EDTA, and 0.05% (w/v) cysteine in a 1:3 ratio (w/v). The homogenate was centrifuged at $1000 \times g$ for 5 min and the supernatant was re-centrifuged for 20 min at $25{,}000 \times g$. The resulting supernatant, assayed as cytosolic fraction, was desalted by dialysis against 50 mM Tris–HCl, pH 7.8 and used for spectrophotometric analysis. The activities of enzymes ascorbate peroxidase (APX; EC 1.11.1.11), catalase (CAT; EC1.11.1.6), peroxidase (POD; EC 1.11.1.7), superoxide dismutase (SOD; EC1.15.11), glutathione reductase (GR; EC 1.6.4.2), dehydroascorbate reductase (DHAR; EC 1.8.5.1) and monodehydroascorbate reductase (MDHAR; EC 1.6.5.4) were tested according to Paciolla et al. (2008) and Mastropasqua et al. (2012). For APX, 1 $U = 1$ nmol of ascorbate oxidized min^{-1}; for CAT, 1 U = 1 nmol of hydrogen peroxide dismutated min^{-1}; for POD, 1 $U = 1$ nmol of 4-methoxy nafthol (MN) oxidized min^{-1}; for SOD, 1 U = the activity of enzyme required to inhibit the reduction rate of nitro blue tetrazolium (NBT) by 50% at 25 °C; for GR, 1 $U = 1$ nmol of nicotinamide adenine dinucleotide phosphate oxidized (NADPH) min^{-1}; for DHAR, 1 $U = 1$ nmol of dehydroascorbate (DHA) reduced min^{-1}; and for MDHAR, 1 $U = 1$ nmol of NADH oxidized min^{-1}. The protein content was determined according to Bradford (1976), using bovine serum albumin as a standard.

Ascorbate and Glutathione Pool Content Determination

Plant samples were homogenized with three volumes of cold 5% (w/v) metaphosphoric acid in a porcelain mortar. The homogenate was centrifuged for 15 min at $20{,}000 \times g$ and the supernatant was collected for the analysis of ascorbate (ASC), dehydroascorbate (DHA), glutathione (GSH) and glutathione oxidized (GSSH) according to Zhang and Kirkham (1996).

Phenol Content Determination

Phenol content was measured by homogenizing 0.5 g of plant samples with 80% ethanol solution in a 1:8 w/v ratio. The homogenate was centrifuged at $7000 \times g$ for 10 min, and to 0.05 mL of supernatant were added 0.95 mL of distilled water and 0.05 mL of a 1:1 water diluted Folin-Ciocâlteu reagent. After 3 min, 100 mL of a 0.1 M NaOH solution containing 20% (w/v) Na_2CO_3 was added, and the mixture was incubated at 25 °C for 90 min in darkness (Singleton et al. 1999). The absorbance was spectrophotometrically measured at $\lambda = 760$ nm. Total phenols were expressed as mg of gallic acid equivalent (GAE) on fresh weight.

Total Antioxidant Content Determination

2,2'-azino-bis(3-ethylbenzothiazoline-6-sulfonic acid) (ABTS) radical-scavenging activity of the hydrophilic fractions was determined by a procedure reported by Teow et al. (2007). Plant samples (0.2 g) were homogenized with 85% ethanol in a 1:6 (w/v) ratio and centrifuged at $20{,}000 \times g$ for 15 min. The total antioxidant activity of supernatant was measured using ABTS as radical reacting with the antioxidant molecules and measuring the absorbance at $\lambda = 730$ nm after 1 min reaction.

H_2O_2 and Lipid Peroxidation Level Determination

H_2O_2 level was evaluated according to Lee and Lee (2000). For lipid peroxidation, plant samples were ground with four volumes of 0.1% (w/v) trichloroacetic acid. The homogenate was centrifuged at $10{,}000 \times g$ for 10 min. One mL of supernatant was diluted with 1 mL of 20% trichloroacetic acid containing 0.5% (w/v) thiobarbituric acid. The level of lipid peroxidation was measured in terms of the malondialdehyde (MDA) content determined by the thiobarbituric acid reaction as described by Zhang and Kirkham (1996).

Statistical Analysis

For gene expression analysis, three biological replicates were considered and plotted values represent the respective means and standard deviation of the means. One-factor analysis of variance (ANOVA), followed by Tukey's HSD test ($p < 0.05$), was performed on the observed means of FC gene expression values to set significant differences between genotypes (CO433 and CO389) within each time of treatment and between times of treatment (3 and 48 h) within each genotype.

For enzymatic activities and compound measurements, four different replicates of four independent experiments

were considered and the error bars represent standard deviation of the means. One-factor ANOVA, followed by Tukey's HSD test ($p < 0.05$), was performed to set significant differences among samples. The statistical package IBM SPSS statistics 27 (IBM Corp., Armonk, NY, USA) was used for data analysis.

Results and Discussion

Fumonisin B_1 is a strong inducer of PCD, and much of the advance in this field was done in the experimental model *A. thaliana* (Iqbal et al. 2021; Zeng et al. 2020). In this regard, Lanubile et al. (2022) reported that FB_1 treatment induced a rapid cell death as well as oxidative and nitrosative bursts in *Arabidopsis* cell cultures. Besides, authors observed a differential modulation of genes involved in PCD regulation, antioxidant metabolism, and pathogenesis, along with glutathione accumulation. This study for the first time extends the use of RNA-Seq and real-time RT-qPCR analysis to identify transcripts related to FB_1 exposure in shoots of resistant and susceptible maize inbred lines. Moreover, biochemical signatures were explored in the same plant material.

Transcriptional Changes in Response to Fumonisin B_1

Transcriptome analysis was carried out at 3 h after FB_1 treatment in the maize genotype CO433, previously classified as resistant to *F. verticillioides* (Maschietto et al. 2016). Sequencing of libraries obtained from maize shoots either buffer (control) and FB_1 treated produced 129,381,999 and 135,886,464 100 bp paired-end reads, respectively, corresponding to about 25.9 Gbps and 27.2 Gbps. Details on paired-end reads statistics for each of the three replicates in each treatment are shown in Supplementary Table 2. On average of 93% of the total reads mapped uniquely to reference Zm-B73-REFERENCE-NAM-v5.0 maize genome sequence. The expression of each of the 44,303 current official maize gene models was extracted as Transcripts Per Kilobase Million (TPM) counts after reads mapping. Eight-thousand three hundred and ten genes had TPM counts equal to zero in all samples. Twenty-six thousand five hundred and forty-four and 27,078 genes were expressed (TPM counts ≥ 0.5) in CO433 genotype after buffer and FB1 treatment, respectively (Supplementary Table 3). Differentially expressed genes between the two treatments were screened by applying an adjusted p-value threshold of 0.05, and logarithmic fold-change threshold values equal to 0.5 and −0.5, revealing a total number of 1,459 genes, of which 1,040 and 419 were up- and down-regulated in the fumonisin treatment, respectively (Supplementary Table 4). To

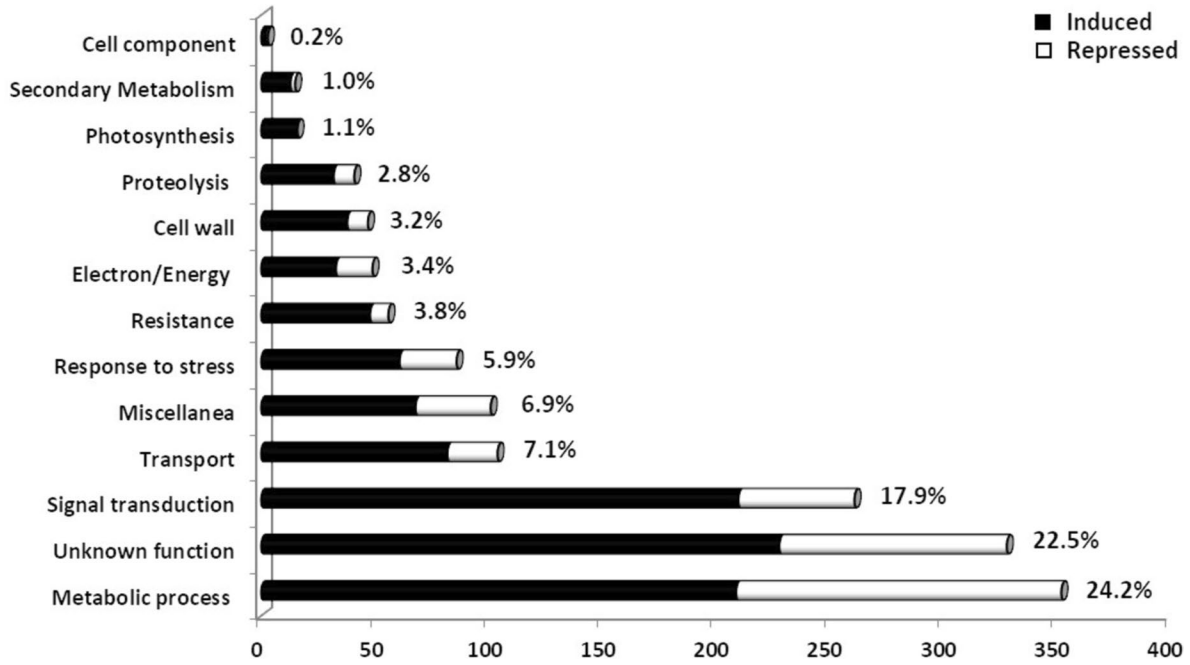

Fig. 1 Functional categories of differentially expressed genes in samples of CO433 genotype at 3 h after fumonisin B_1 (FB_1) treatment. Induced genes are represented in black, while repressed ones are in white. The total percentage of modulated transcripts within each functional category is also shown. The complete list of genes is available in Supplementary Table 4

better understand their functionality, DEGs were annotated using Blast2GO software (Götz et al. 2008) and classified in 13 broader functional categories (Fig. 1; Supplementary Table 4).

After removing genes with unassigned function, the largest proportion of DEGs belonged to metabolic process (24.2%), signal transduction (17.9%) and defense-related functional classes (13.9% in total), such as resistance, response to stress, cell wall and secondary metabolism. These last classes consisted of several DEGs encoding putative thaumatin-like proteins, metacaspases, heat shock proteins, and pectinesterases, the majority of them induced after fumonisin exposure and with a pectin methyltransferase showing the highest log2FC values of 10.3 (Fig. 1; Supplementary Table 4). Besides these two classes, the second largest group of DEGs was related to signal transduction and included several genes encoding putative transcription factors as those belonging to AP2 (APETALA2)-EREBP (ethylene-responsive element binding proteins), MYB, NAC, WRKY and TIFY families (Supplementary Table 4).

To gain more insight into the potential mechanisms underlying cell death caused by FB_1 exposure, the analysis of transcriptional changes for a set of twelve genes involved in the antioxidant metabolism, mycotoxin detoxification, PCD regulation, hormone signaling, and ubiquitination, was extended by RT-qPCR at 3 and 48 h in the resistant and susceptible genotypes CO433 and CO389, respectively (Fig. 2). Ten genes resulted as differentially regulated from RNA-Seq investigation (Supplementary Table 4) and an exact agreement between the two techniques was found. Further two genes encoding for *ascorbate peroxidase* (*APX*) and *catalase* (*CAT*), previously considered along with *superoxide dismutase* (*SOD*) as markers for the stress response to several fungal pathogens (Maschietto et al. 2016; Lanubile et al. 2015, 2017), were included in the panel of genes to be monitored in the wider expression analysis. The relative

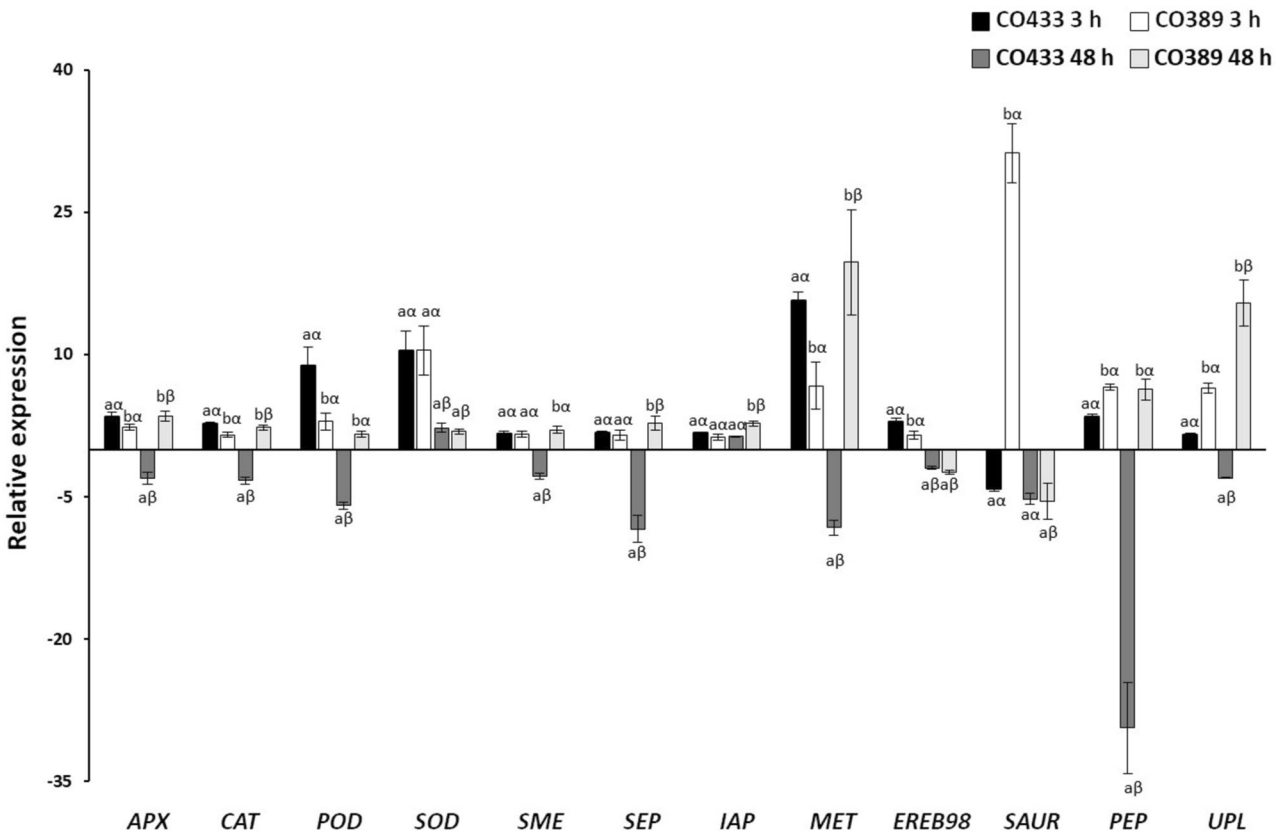

Fig. 2 RT-qPCR analysis of *Zea mays* genes upon fumonisin B_1 (FB_1) treatment. Relative expression between FB_1 and buffer treated samples of CO433 and CO389 genotypes (black and white bar graphs, respectively) for 3 and 48 h. *ascorbate peroxidase* (*APX*); *catalase* (*CAT*); *peroxidase* (*POD*); *superoxide dismutase* (*SOD*); *small multi-drug export protein* (*SME*); *stress enhanced protein chloroplastic-like* (*SEP*); *inhibitor of apoptosis-like protein* (*IAP*); *metacaspase* (*MET*); *AP2-EREBP-transcription factor 98* (*EREB*); *SAUR33-auxin-responsive SAUR family member* (*SAUR*); *prolyl endopeptidase* (*PEP*); *ubiquitin-protein ligase* (*UPL*). Vertical bars indicate ± sd. The same letters over the bar graphs state not significant differences between means of the two genotypes (CO433 and CO389) within each time of treatment (3 and 48 h) (Latin letters) and the two times of treatment within each genotype (Greek letters), as resulting from Tukey's honestly significant difference test ($p < 0.05$). Experiments refer to three independent biological replicates. Bars indicate the mean and error bars indicate the SD

expression profiles were calculated as fold change (FC) of FB_1 over buffer treated samples.

Regarding genes protecting from oxidative stress, transcripts encoding *APX*, *CAT*, *SOD*, and *peroxidase* (*POD*), all showed increased expression levels for both genotypes at early FB_1 treatment time, more enhanced in CO433, with the exception of *SOD* where no significant differences between genotypes were observed (FC of about 10.4 for both inbred lines; Fig. 2). At late exposure time *APX*, *CAT*, and *POD* were down-regulated in CO433, whereas the susceptible line displayed a higher induction in the expression level of 3.5 and 2.3-fold for *APX* and *CAT*, respectively. Once again, no significant variation was displayed by *SOD* between CO433 and CO389 at this treatment time (Fig. 2).

The production of reactive oxygen species (ROS) is rapidly induced in host plant after recognition of a pathogen or elicitor like FB_1, and its accumulation was previously reported in several plant species (*A. thaliana*, tobacco, tomato, and maize) and target organs (leaves, root, seedlings, and cell cultures) (Harvey et al. 2008; Lanubile et al. 2022; Otaiza-González et al. 2022; Qin et al. 2017; Stone et al. 2000; Wu et al. 2015; Xing et al. 2013; Zhao et al. 2015). A key role in ROS detoxification is carried out by antioxidant enzymes as SOD that catalyses the conversion of O_2^- to O_2 and H_2O_2 (Alscher et al. 2002). The latter is degraded by the concerted action of peroxisome-localised CAT, cytosolic or chloroplastic APX, along with POD (Czarnocka and Karpinski 2018).

It was reported that the antioxidant gene *APX* displayed an abundant transcript accumulation in *Arabidopsis* cells during the late FB_1 treatment time more enhanced at higher fumonisin concentrations (Lanubile et al. 2022). Iqbal et al. (2023) described a significant induction of *SOD-CuZn*, *SOD-Mn*, *CAT2* and *CAT3* isoforms along with *APX1* and *APX2* in fusaric acid treated tomato seedlings particularly after 72 h exposure, whereas *SOD-Fe* and *CAT1* genes were down-regulated throughout the examined time-course. Moreover, transcripts encoding a class III plant *POD* increased at higher levels in wheat coleoptiles of a deoxynivalenol resistant cultivar but not in the susceptible one (Ansari et al. 2014).

For the successful survival to mycotoxin exposure, plants have to activate not only their antioxidant system to reduce ROS effects, but also utilize detoxification approaches to attenuate the impact of toxin accumulation. In this regard, the expression of a gene encoding for a *small multi-drug export protein* (*SME*) was also evaluated deeper in response to FB_1 in different genotypes and at different time points upon treatment (Fig. 2). Again, a down-regulation occurred in the resistant genotype CO433 at late treatment time (FC of −2.8) differently from the susceptible genotype, whereas it did not show any significant transcriptional change between 3 and 48 h in the CO389 line (Fig. 2).

The exposure to FB_1 also initiates PCD in a process involving multiple pathways such as the activation of specific plant proteases and nucleases causing DNA fragmentation (Zeng et al. 2020). The transcriptional changes of three genes related to PCD regulation were also considered in this work (Fig. 2). All three genes were up-regulated in the CO433 line at 3 h with FC ranging from 1.7 for the gene encoding an *inhibitor of apoptosis-like protein* (*IAP*) to 15.7 for the *metacaspase* (*MET*), whereas more attenuated or even repressed levels of transcripts were observed at late timepoint. An opposite trend was found for the susceptible line CO389 where FB_1 treatment resulted in a lower expression at early timepoint followed by an increase after 48 h, with the highest gene induction for *MET* (FC of 19.7). Metacaspases are a class of cysteine-dependent proteases that orchestrate cell suicide and plant defense responses. In maize, the localization of *MET* with previously identified quantitative trait loci (QTL) associated to disease resistance showed that most of them co-localize with at least one QTL for resistance to southern and northern leaf blight, grey leaf spot or Fusarium ear rot (Ma et al. 2021). Different modulation levels of *MET* were found against *Cochliobolus heterostrophus* and *F. verticillioides* by RNA-Seq analysis (Ma et al. 2021).

It was observed that the metacaspase-coding sequences like *AtMC3*, *AtMC8*, and *AtMC9* were also expressed within 24 h upon 10 µM FB_1 infiltration of 6-week-old *Arabidopsis* leaves (Kwon and Hwang 2013). Moreover, the degree of cell death decreased in tomato cell suspension exposed to FB_1 after treatment with caspase (lysophosphatidyl ethanolamine) and serine protease (4-(2-aminoethyl) benzenesulfonyl fluoride hydrochloride) inhibitors (Iakimova et al. 2004, 2013).

Caspase activation is prevented by the inhibitor of apoptosis IAP. The transgenic expression of *IAP* in tomato determined resistance to lesions caused by FB_1 (Li et al. 2010), and an enhanced antiapoptotic activity resulted in *Arabidopsis IAP* overexpressing plants when exposed to FB_1 (Kim et al. 2011). Recently, Lanubile et al. 2022 reported that *Arabidopsis* cell cultures displayed *IAP* induction especially 48 h after fumonisin treatment more enhanced at 5 µM compared to lower concentrations, confirming the role of this gene as PCD mediator in several species.

Plant susceptibility to FB_1 is well known to be associated with hormone signaling. In this regard, the expression profiles of genes encoding *AP2-EREBP-transcription factor 98* (*EREB*) and *SAUR33-auxin-responsive* (*SAUR*) were tested (Fig. 2). *EREB* was induced in both genotypes at 3 h, but to a more marked extent in the resistant line CO433 (FC = 2.9), whereas a down-regulation characterized the late time of FB_1 treatment with FC of −1.9 and −2.4 for CO433 and CO389, respectively (Fig. 2). A similar pattern was displayed by

SAUR in the two genotypes at late timepoint. Interestingly, the gene was also negatively regulated of 4.2-fold at 3 h in the resistant line (Fig. 2), suggesting that it could act as a susceptibility factor whose induction would favour more likely PCD progress rather than its containment. In line with this, Wang et al. (2012) reported the down-regulation of five genes associated to the auxin pathway in *Arabidopsis* leaves after ochratoxin A treatment. Moreover, it was demonstrated that FB_1 restricts *Arabidopsis* root growth by reducing the expression of several PIN-FORMED auxin carriers (Zhao et al. 2022). Expression experiments of additional auxin-associated genes and functional studies with plant mutants should help to better understand how this hormone participates in the FB_1-induced cell death.

By contrast, a higher number of works focused on the role of the hormone ethylene in plant responses to FB_1 and mycotoxins in general are available. It was found that *Arabidopsis* mutants having defective ethylene biosynthesis or signaling presented a more elevated chlorophyll degradation and cell death boosting (Plett et al. 2009). In addition, the ethylene receptor mutant *Never ripe* of tomato showed a more abundant activation of antioxidant enzymes such as SOD, APX and glutathione S-transferase compared to wild-type plants (Iqbal et al. 2023). However, Mase et al. (2013) observed also an increased expression of *ethylene response factor 1* and *102* within 24 h in FB_1-treated *Arabidopsis* leaves. Interestingly, FB_1-induced PCD was significantly reduced by exogenous treatment with ethylene precursor 1-aminocyclopropane-1-carboxylic acid (ACC) (Wu et al. 2015), and an enhanced transcript accumulation of *ACC oxidase* was observed in the late times of fumonisin exposure in *Arabidopsis* (Lanubile et al. 2022).

Plant hormone signaling is also regulated by the ubiquitin–proteasome complex (Santner and Estelle 2010). The expression of two genes that may play a role in this process was considered in this study: the *prolyl endopeptidase* (*PEP*) and the *ubiquitin-protein ligase* (*UPL*) (Fig. 2). Both genes were induced in the CO433 line at 3 h, whereas a down-regulation occurred at 48 h. Conversely, transcript accumulation of *PEP* and *UPL* was maintained high in the susceptible genotype CO389 throughout the time course. The ubiquitination pathway is required for protein recycling with the aim to maintain protein balance in response to several stimuli including plant–microbe interactions (Zeng et al. 2006).

Different transcripts directly implicated in the ubiquitination process or acting as regulatory or structural elements of the proteasomal system accumulated in barley after *F. graminearum*-derived trichothecene accumulation (Boddu et al. 2007) as well as in *Arabidopsis* leaves in response to ochratoxin A treatment (Wang et al. 2012). Furthermore, the ubiquitin ligases ring domain ligase 3 (RGLG3) and RGLG4 coordinately and positively regulated FB_1-triggered PCD by suppressing salicylic acid and modulating jasmonic acid signaling pathway in *Arabidopsis* (Zhang et al. 2015). Similarly, the pepper E3 ubiquitin ligase *RING1* gene was required for cell death and the salicylic acid-mediated defense responses (Lee et al. 2011), emphasizing the role of this gene category in regulating PCD along with hormone crosstalk.

Oxidative Status Regulation in Response to Fumonisin B_1

Different enzymes and compounds involved in the oxidative burst and ROS detoxification processes were considered in this study to assess the effect of FB_1 on the antioxidant activities of resistant and susceptible maize genotypes (Figs. 3 and 4).

In the line CO433, a strong correlation was found between the trend of gene expression and that of enzymatic activity of APX, CAT, POD and SOD at both treatment times (Fig. 3A–D).

Particularly, at 3 h an augmented expression and activity of these enzymes was observed, whereas at 48 h a contemporaneous drop of both occurred, highlighting an earlier activation of defense responses in the resistant genotype. The contemporaneous increase of APX and SOD after 3 h of FB_1 treatment underlined the presence of an efficient mechanism of superoxide anion removal, the latter a reactive oxygen species strongly toxic for plant cell. In CO433, the higher accumulation of hydrogen peroxide (H_2O_2) observed, potentially toxic for cell, can be due in part to the increased dismutation reaction of the toxic O_2- catalyzed by SOD enzyme (Fig. 3D, E).

However, H_2O_2 presence was counteracted by a higher APX activity along with an ASC increase (Figs. 3A and 4A, respectively) that participate in this reaction by supplying reducing equivalents (Paciolla et al. 2019).

Furthermore, the early enhanced levels of CAT and POD, the other enzymes utilizing and scavenging H_2O_2, contributed to avoid its higher and toxic accumulation (Fig. 3B, C). In addition, the parallel decrease of GSH observed in the first hours after treatment (3 h) underlined the prompt availability of ASC than GSH one, the other antioxidant metabolite of the cycle, indicating an earlier activation of ascorbate biosynthetic pathway rather than GSH one, in the complex ascorbate–glutathione cycle (Fig. 4B; Foyer and Noctor 2011). This trend confirmed the known primary role of the ascorbate system in the defense responses (Foyer and Noctor 2005). On the other side, the reduction of GR activity, enzyme of GSH reconversion by GSSG (Sabetta et al. 2017), further supported this behavior (Fig. 4C). Interestingly, the non-involvement of the enzymes of reconversion of DHA to ASC, namely DHAR and MDHAR (Loi et al. 2020a, b), whose activity decreased, pointed out an *ex novo* synthesis of ASC (Fig. 4D, E).

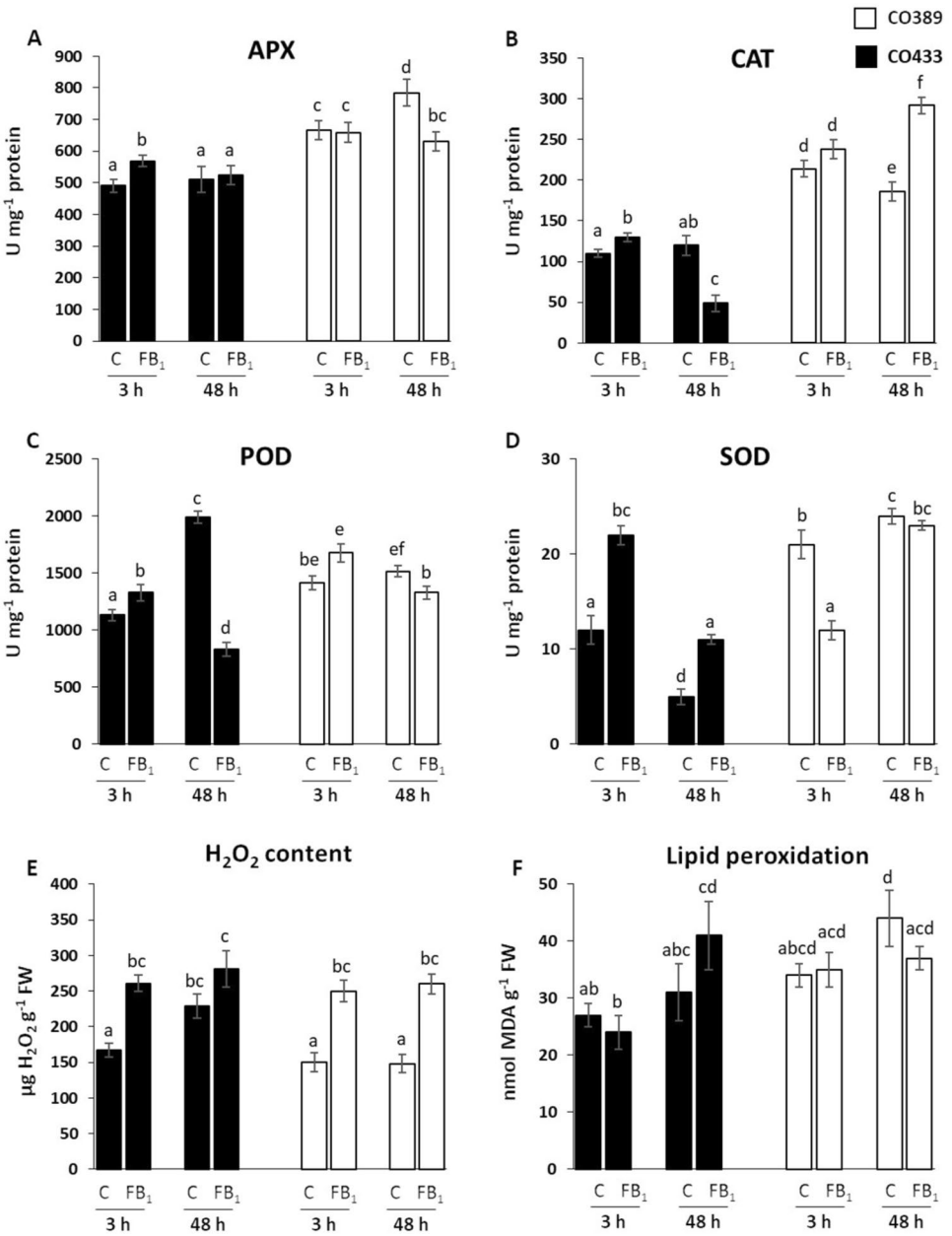

Fig. 3 Enzyme activity of **A** ascorbate peroxidase (APX), **B** catalase (CAT), **C** peroxidase (POD), **D** superoxide dismutase (SOD), and production of **E** hydrogen peroxide (H_2O_2) and **F** malondialdehyde (MDA) in buffer (control, C) and fumonisin B_1 (FB_1) treated samples of CO433 and CO389 genotypes (black and white bars, respectively) for 3 and 48 h. One unit (U) of enzyme activity corresponds to 1 nmol of the substrate metabolized in 1 min. FW: Fresh Weight. Vertical bars indicate ± sd. Different letters over the bar graphs indicate significant differences among samples, as resulting from Tukey's honestly significant difference test ($p < 0.05$). Experiments refer to four independent biological replicates. Bars indicate the mean and error bars indicate the SD

At later treatment time (48 h), even though a decrease of CAT and POD activities occurred (Fig. 3B, C), a non significant change in the H_2O_2 content and lipid peroxidation level was found (Fig. 3E, F). This was probably due to a valuable APX activity after FB_1 treatment that did not change compared to the control (Fig. 3A). It is known that APX, CAT and POD are enzymes contributing to control the H_2O_2 level in the cell. A decrease in their activity could lead to an increase of hydrogen peroxide and possible damage to the biological membranes with consequent increase in peroxidation lipid level. On the other hand, due to its higher affinity for H_2O_2 than CAT and POD (Paciolla et al. 2016), APX was able to counteract H_2O_2 accumulation after FB_1 treatment.

The enhancement of GR and DHAR enzymes did not cause any decrease in GSH and ASC compared to the control samples (Fig. 4A–D). DHAR has a key role in maintaining the reduced levels of ASC avoiding DHA degradation (Gallie, 2013) and GR has an important role in keeping the normal balance between reduced GSH and ASC pools (Ding et al., 2009). SOD enzyme maintained higher its activity also at 48 h (Fig. 3D).

Besides H_2O_2 scavenging and ascorbate–glutathione cycle enzymes and components, total antioxidants and phenols were measured in this work (Fig. 4F, G). At early

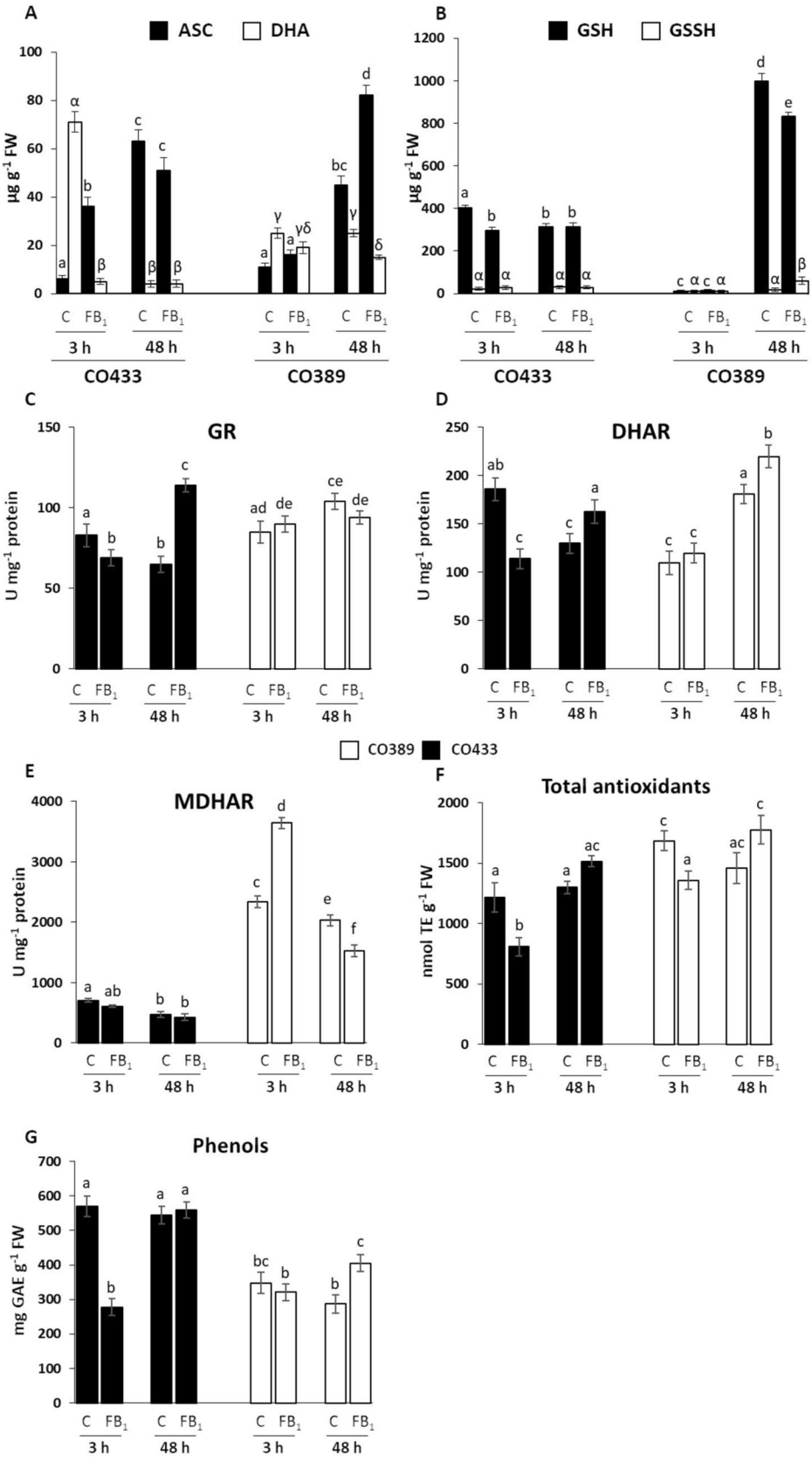

Fig. 4 Production of compounds involved in the ascorbate–glutathione cycle **A** ascorbate (ASC) and dehydroascorbate (DHA) (black and white bars, respectively), and **B** glutathione (GSH) and glutathione oxidized (GSSH) (black and white bars, respectively), enzyme activity of **C** glutathione reductase (GR), **D** dehydroascorbate reductase (DHAR) and **E** monodehydroascorbate reductase (MDHAR), and content of **F** total antioxidants and **G** phenols in buffer (control, C) and fumonisin B_1 (FB_1) treated samples of CO433 and CO389 genotypes (black and white bars, respectively) for 3 and 48 h. One unit (U) of enzyme activity corresponds to 1 nmol of the substrate metabolized in 1 min. TE: Trolox Equivalents; GAE: Gallic Acid Equivalents; FW: Fresh Weight. Vertical bars indicate ± sd. Different letters over the bar graphs indicate significant differences among samples, as resulting from Tukey's honestly significant difference test ($p < 0.05$). As regards the ascorbate–glutathione cycle compounds, different Latin and Greek letters over the bar graphs indicate significant differences among samples for the compounds ASC and GSH, and DHA and GSSH, respectively. Experiments refer to four independent biological replicates. Bars indicate the mean and error bars indicate the SD

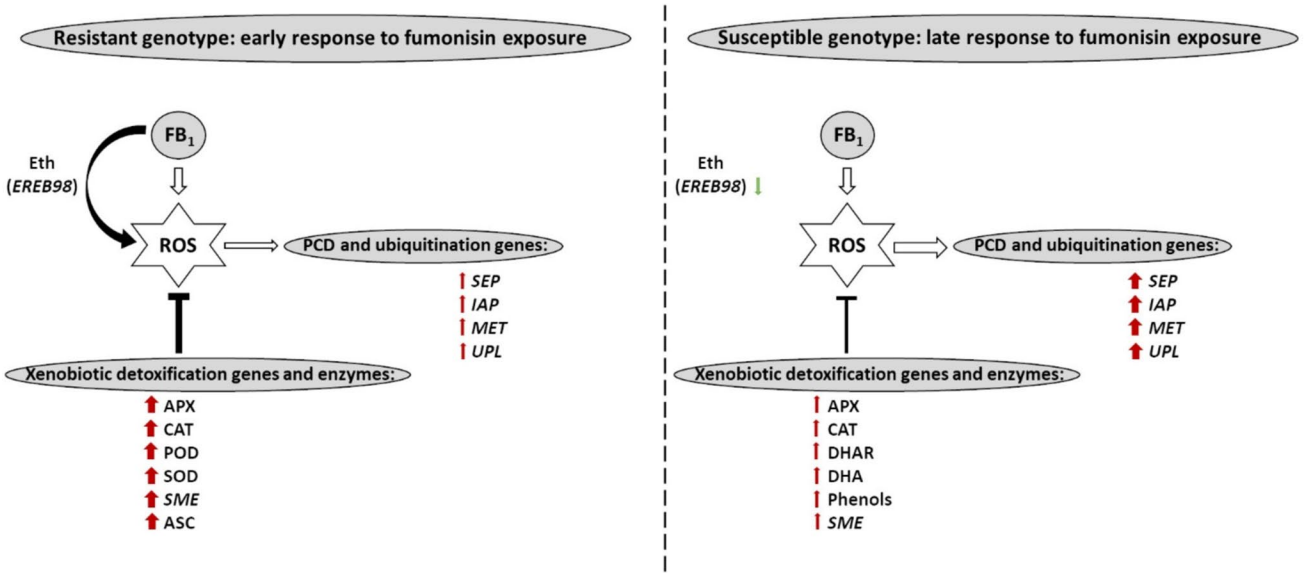

Fig. 5 Hypothetical model of the transcriptional and biochemical effects of fumonisin B_1 (FB_1) on the resistant (CO433) and susceptible (CO389) maize shoots at early (3 h) and late (48 h) stages after treatment. Weak and strong responses are denoted by thinner and thicker arrows, respectively. Moreover, red or green arrows indicate the increase and decrease of the different components, respectively. Eth, ethanol; *EREB98, AP2-EREBP-transcription factor 98*; ROS, reactive oxygen species; APX, ascorbate peroxidase; CAT, catalase; POD, peroxidase; SOD, superoxide dismutase; *SME, small multidrug export protein*; ASC, ascorbate; *SEP, stress enhanced protein chloroplastic-like*; *IAP, inhibitor of apoptosis-like protein*; *MET, metacaspase*; *UPL, ubiquitin-protein ligase*; DHAR, dehydroascorbate reductase; DHA, dehydroascorbate

treatment time, the production of both compounds was significantly fallen in the resistant line, whereas at longer time raised (total antioxidants, Fig. 4F) or remained unchanged (phenols, Fig. 4, G). This opposite trend suggests the presence of possible endogen mechanisms useful to balance and maintain the antioxidant capacity of the cell system in a steady state (Paciolla et al. 2016).

Concerning the susceptible line CO389, in general the activities of H_2O_2 scavenging enzymes correlated in a less marked way to the gene expression pattern. At 3 h from the treatment with FB_1 fewer striking differences were observed in the activities of APX, CAT and POD in comparison with the control samples (Fig. 3A–C), except for SOD, where a significant reduction was found (Fig. 3D). The augmented H_2O_2 levels after FB_1 exposure at 3 and 48 h were not supported by an increase in SOD activity, suggesting that other processes, such as photorespiration, might contribute to the H_2O_2 production (Fig. 3E; Noctor et al. 2002). In a recent study, Otaiza-González et al. (2022) explored the FB_1 phytotoxicity in two maize hybrids with contrasting phenotypes to Fusarium ear rot. In general, both hybrids showed an activation of several oxidative status biomarkers in seedlings treated with FB_1 over a time-course of 21 days. However, using a hydroponic model at 24 h after exposure the mycotoxin caused a decrease in the activities of SOD and guaiacol POD in the susceptible hybrid, whereas the opposite was detected in the resistant plants highlighting the complexity of FB_1-induced signaling network in plants.

Regarding the two enzymes involved in the reconversion of DHA in ASC, whereas MDHAR increased its activity at 3 h and decreased a 48 h, DHAR did not change at 3 h and increased at 48 h from the treatment, underlining the presence of a different action timing for these two enzymes (Fig. 4D, E). This enzymatic trend favored the reduction of DHA that at longer time significantly decreased, while in contrast a corresponding ASC increment occurred (Fig. 4A).

The weak GR increase and decrease at 3 and 48 h, respectively, did not contribute positively to the GSH recovery that at later time-point significantly dropped (Fig. 4B, C). In addition, the parallel higher GSSH production contributed to shift the redox state of this metabolite versus the oxidative form (Fig. 4B; Sabetta et al. 2017). On the other hand, the reduction of APX and POD activities after 48 h further contributed to the higher oxidized cell status. In the susceptible line, however, together with an ASC increase, the positive involvement of other compounds in the cell defense system was observed at 48 h (Fig. 4F, G). Indeed, the augmented content of phenolic compounds as well as the increased CAT activity levels appeared as a tentative to control the significant accumulation of H_2O_2, speculating the attempt of the CO389 genotype to counteract the metabolic perturbations induced by FB_1.

The induction of oxidative burst by FB_1 was previously explored in other species (Iqbal et al. 2021). *Arabidopsis* plants elicited with 10 µm FB_1 mounted an HR that included the generation of ROS intermediates, the accumulation of phenols, callose and phytoalexins, as well as the expression of *PR* genes (Stone et al. 2000). Antioxidant enzymatic defense mechanisms were also activated by FB_1 in tomato plants in an ethylene-dependent manner, where increased levels of SOD, APX and gluthathione-S-transferase activities were reported (Iqbal et al. 2022). Similar effects were observed in the same tomato genotypes after fusaric acid treatment (Iqbal et al. 2023; 2024). Moreover, an elevated content of ROS and MDA was measured in *Arabidopsis* leaves after ochratoxin A treatment, whereas deoxynivalenol exposure induced PCD supported by ROS generation along with a mitochondrial disfunction in tobacco cells (Yekkour et al. 2015).

The antioxidant response is not the only mechanism of tolerance to *Fusarium* spp. and their mycotoxins production. Six major groups of compounds derived from plant primary and secondary metabolism and potentially able to counteract toxigenic *Fusaria* and mycotoxins accumulation in cereals were described, and included fatty acids, aminoacids and derivatives, carbohydrates, amines and polyamines, terpenoids and phenylpropanoids (Gauthier et al. 2015). Further studies investigated the impact of α-tocopherol and carotenoids on mycotoxin production, and highlighted how these two metabolites significantly affected the production of fumonisins (Picot et al. 2013) and type B trichothecene (Atanasova-Penichon et al. 2016), respectively. Additional experiments focusing on the metabolite composition of resistant and susceptible genotypes challenged or not with FB_1 will clarify our findings more accurately in light of these previous studies.

Conclusion

In summary, in this work, it was shown that albeit FB_1 exposure did not cause shoot suffering in both resistant and susceptible maize lines, it resulted in notably different transcriptional and biochemical perturbations (Fig. 5). Defense responses promptly appeared activated in the shoots of CO433 genotype. More in detail, at 3 h after treatment, FB_1 induced ROS generation, particularly H_2O_2, whose accumulation was hindered by the enhanced expression and activities of genes and enzymes involved in the xenobiotic detoxification processes (*APX*, *CAT*, *POD*, *SOD* and *SME*), and combined with a higher content of ASC. Moreover, ROS accumulation, probably mediated by an ethylene-dependent signaling transduction pathway, determined an upregulation of genes engaged in PCD regulation (*SEP*, *IAP* and *MET*) and ubiquitination (*PEP* and *UPL*) events. In contrast, in the CO389 susceptible line, most of assayed genes, enzymes and compounds increased their levels only at later treatment time, conferring a lower readiness in response to the mycotoxin. A weaker attempt to counteract ROS production was supplied by the xenobiotic detoxification genes and enzymes, thus determining a higher accumulation of transcripts associated to PCD and ubiquitination processes.

These data provide useful key candidate genes and biomarkers for the detection of FB_1 exposure and could speed up the development of successful plant protection and disease management strategies also towards other mycotoxins.

Supplementary Information The online version contains supplementary material available at https://doi.org/10.1007/s00344-024-11564-9.

Acknowledgements The authors would like to thank Dr. Silvana De Leonardis (Department of Biosciences, Biotechnology and Environment, Università degli Studi di Bari Aldo Moro, Bari, Italy), Dr. Giuseppe Cozzi (Institute of Sciences of Food Production, CNR, Bari, Italy) for technical help, and Prof. Massimo Delledonne at the Functional Genomics Center of the Biotechnology, Department of the University of Verona, where sequencing of RNA libraries was conducted.

Author Contributions Conceptualization, AL, DB, AM, GM and CP; investigation, AL, DB, LO, MJ and CP; writing–original draft preparation, AL and CP; writing–review and editing, AL, DB, LO, MJ, AM, GM and CP.

Funding This work was financially supported by PRIN 20094CEKT4 of the MIUR, Italy and by H2020-E.U.3.2–678781-MycoKey-Integrated and innovative key actions for mycotoxin management in the food and feed chain. Università Cattolica del Sacro Cuore contributed to the funding of this research project and its publication.

Declarations

Conflict of interest No conflict of interest is declared.

References

Alscher RG, Erturk N, Heath LS (2002) Role of superoxide dismutases (SODs) in controlling oxidative stress in plants. J Exp Bot 53:1331–1341

Ansari KI, Doyle SM, Kacprzyk J et al (2014) Light influences how the fungal toxin deoxynivalenol affects plant cell death and defense responses. Toxins 6:679–692

Asai T, Stone JM, Heard JE et al (2000) Fumonisin B1–induced cell death in *Arabidopsis* protoplasts requires jasmonate-, ethylene-, and salicylate-dependent signaling pathways. Plant Cell 12:1823–1835

Atanasova-Penichon V, Barreau C, Richard-Forget F (2016) Antioxidant secondary metabolites in cereals: potential involvement in resistance to *Fusarium* and mycotoxin accumulation. Front Microbiol 7:566

Baldwin TT, Zitomer NC, Mitchell TR et al (2014) Maize seedling blight induced by *Fusarium verticillioides*: accumulation of fumonisin b 1 in leaves without colonization of the leaves. J Agric Food Chem 62:2118–2125

Benjamini Y, Hochberg Y (1995) Controlling the false discovery rate: a practical and powerful approach to multiple testing. J R Stat Soc Series B Stat Methodol 57:289–300

Boddu J, Cho S, Muehlbauer GJ (2007) Transcriptome analysis of trichothecene-induced gene expression in barley. Mol Plant-Microbe Interact 20:1364–1375

Bradford MM (1976) A rapid and sensitive for the quantitation of microgram quantitites of protein utilizing the principle of protein-dye binding. Anal Biochem 72:248–254

Czarnocka W, Karpinski S (2018) Friend or foe? reactive oxygen species production, scavenging and signaling in plant response to environmental stresses. Free Radic Biol Med 122:4–20

Desjardins AE, Plattner RD, Nelsen TC et al (1995) Genetic analysis of fumonisin production and virulence of *Gibberella fujikuroi* mating population A (*Fusarium moniliforme*) on maize (*Zea mays*) seedlings. Appl Environ Microbiol 61:79–86

Di Tommaso P, Chatzou M, Floden EW et al (2017) Nextflow enables reproducible computational workflows. Nature Biotechnol 35:316–319

Dobin A, Davis CA, Schlesingeret F et al (2013) STAR: ultrafast universal RNA-seq aligner. Bioinformatics 29:15–21

Food and Agriculture Organization of the United Nations (2021) Agricultural production statistics. 2000–2021. FAOSTAT Analytical Brief Series No. 60. Rome

Foyer CH, Noctor A (2005) Oxidant and antioxidant signalling in plants: are-evaluation of the concept of oxidative stress in a physiological context. Plant Cell Environ 28:1056–1071

Foyer CH, Noctor G (2009) Redox regulation in photosynthetic organisms: signaling, acclimation, and practical implications. Antioxidants Redox Signal 11:861–905

Foyer CH, Noctor G (2011) Ascorbate and Glutathione: the heart of the redox hub. Plant Physiol 155:2–18

Gauthier L, Atanasova-Penichon V, Chéreau S et al (2015) Metabolomics to decipher the chemical defense of cereals against *Fusarium graminearum* and deoxynivalenol accumulation. Int J Mol Sci 16:10

Götz S, Garcia-Gomez JM, Terol J et al (2008) High-throughput functional annotation and data mining with the Blast2GO suite. Nucleic Acids Res 36:3420–3435

Harvey JJ, Lincoln JE, Gilchrist DG (2008) Programmed cell death suppression in transformed plant tissue by tomato cDNAs identified from an *Agrobacterium rhizogenes*-based functional screen. Mol Genet Genom 279:509–521

Iakimova ET, Batchvarova R, Kapchina-Toteva V et al (2004) Inhibition of apoptotic cell death induced by *Pseudomonas syringae* pv. *tabaci* and mycotoxin Fumonisin B1. Biotechnol Biotechnol Equip 18:34–46

Iakimova ET, Michaeli R, Woltering EJ (2013) Involvement of phospholipase D related signal transduction in chemical-induced programmed cell death in tomato cell cultures. Protoplasma 250:1169–1183

International Agency for Research on Cancer (1993) Monographs on the evaluation of carcinogenic risks to humans: some naturally occurring substances: food items and constituents, heterocyclic aromatic amines and mycotoxins. Lyon, France: International Agency for Research on Cancer 56:1–599

Iqbal N, Czékus Z, Poór P et al (2021) Plant defence mechanisms against mycotoxin fumonisin B1. Chem Biol Interac 343:109494

Iqbal N, Czékus Z, Angeli C et al (2022) Fumonisin B1-induced oxidative burst perturbed photosynthetic activity and affected antioxidant enzymatic response in tomato plants in ethylene-dependent manner. J Plant Growth Regul 42:1865–1878

Iqbal N, Czékus Z, Poór P et al (2023) Ethylene-dependent regulation of oxidative stress in the leaves of fusaric acid-treated tomato plants. Plant Physiol Biochem 196:841–849

Iqbal N, Czékus Z, Ördög A et al (2024) Fusaric acid-evoked oxidative stress affects plant defence system by inducing biochemical changes at subcellular level. Plant Cell Rep 43:2

Ismaiel A, Papenbrock J (2015) Mycotoxins: producing fungi and mechanisms of phytotoxicity. Agriculture 5:492–537

Kim WY, Lee SY, Jung YJ et al (2011) Inhibitor of apoptosis (IAP)-like protein lacks a baculovirus IAP repeat (BIR) domain and attenuates cell death in plant and animal systems. J Biol Chem 286:42670–42678

Kwon SI, Hwang DJ (2013) Expression analysis of the metacaspase gene family in *Arabidopsis* J. Plant Biol 56:391–398

Lanubile A, Logrieco A, Battilani P et al (2013) Transcriptional changes in developing maize kernels in response to fumonisin-producing and nonproducing strains of *Fusarium verticillioides*. Plant Sci 210:183–192

Lanubile A, Machietto V, Marocco A (2014) Breeding maize for resistance to mycotoxins. In: Logrieco AF (ed) Mycotoxin reduction in grain chains; Leslie JF. Wiley Blackwell, Oxford, UK, pp 37–58

Lanubile A, Maschietto V, De Leonardis S et al (2015) Defense responses to mycotoxin-producing fungi *Fusarium proliferatum*, *F. subglutinans*, and *Aspergillus flavus* in kernels of susceptible and resistant maize genotypes. Mol Plant Microbe Interact 28:546–557

Lanubile A, Maschietto V, Battilani P et al (2017) Infection with toxigenic and atoxigenic strains of *Aspergillus flavus* induces different transcriptional signatures in maize kernels. J Plant Interact 12:21–30

Lanubile A, De Michele R, Loi M et al (2022) Cell death induced by mycotoxin fumonisin B1 is accompanied by oxidative stress and transcriptional modulation in *Arabidopsis* cell culture. Plant Cell Rep 41:1733–1750

Lee DH, Lee CB (2000) Chilling stress-induced changes of antioxidant enzymes in the leaves of cucumber: in gel enzyme activity assays. Plant Sci 159:75–85

Lee DH, Choi HW, Hwang BK et al (2011) The pepper E3 ubiquitin ligase RING1 gene, CaRING1, is required for cell death and the salicylic acid-dependent defense response. Plant Physiol 156:2011–2025

Li H, Handsaker B, Wysoker A et al (2009) The sequence alignment/map format and SAMtools. Bioinformatics 25:2078–2079

Li W, Kabbage M, Dickman MB (2010) Transgenic expression of an insect inhibitor of apoptosis gene, SfIAP, confers abiotic and biotic stress tolerance and delays tomato fruit ripening. Physiol Mol Plant Pathol 74:363–375

Logrieco A, Battilani P, Camardo Leggieri M et al (2021) Perspectives on global mycotoxin issues and management from the mycokey maize working group. Plant Dis 105:525–537
Loi M, Paciolla C, Logrieco AF et al (2020a) Plant bioactive compounds in pre- and postharvest management for aflatoxins reduction. Front Microbiol 11:243
Loi M, Leonardis S, Mulè G et al (2020b) A novel and potentially multifaceted dehydroascorbate reductase increasing the antioxidant systems is induced by beauvericinin tomato. Antioxidants (Basel) 9:435
Love MI, Huber W, Anders S (2014) Moderated estimation of fold change and dispersion for RNA-seq data with DESeq2. Genome Biol 15:550
Ma S, Shi H, Wang GF (2021) The potential roles of different metacaspases in maize defense response. Plant Signal Behav 16:1906574
Martin M (2011) Cutadapt removes adapter sequences from high-throughput sequencing reads. EMBnet.journal 17:10–12
Maschietto V, Lanubile A, De Leonardis S et al (2016) Constitutive expression of pathogenesis-related proteins and antioxydant enzyme activities triggers maize resistance towards *Fusarium verticillioides*. J Plant Physiol 200:53–61
Mase K, Ishihama N, Mori H et al (2013) Ethylene-responsive AP2/ERF transcription factor MACD1 participates in phytotoxin-triggered programmed cell death. Mol Plant Microbe Interact 26:868–879
Mastropasqua L, Borraccino G, Bianco L et al (2012) Light qualities and dose influence ascorbate pool size in detached oat leaves. Plant Sci 183:57–64
Munkvold GP, Proctor RH, Moretti A (2021) Mycotoxin production in *Fusarium* according to contemporary species concepts. Annu Rev Phytopathol 59:373–402
Nishimura MT, Stein M, Hou BH et al (2003) Loss of a callose synthase results in salicylic acid-dependent disease resistance. Science 301:969–972
Noctor G, Veljovic-jovanovis S, Driscoll S et al (2002) Drought and oxidative load in the leaves of C3 plants: a predominant role for photorespiration? Ann Bot 89:841–850
Noctor G, Reichheld JP, Foyer CH (2018) ROS-related redox regulation and signaling in plants, in: Seminars in Cell & Developmental Biology 80, Academic Press, pp. 3–12
Otaiza-González SN, Mary VS, Arias SL et al (2022) Cell death induced by fumonisin B1 in two maize hybrids: correlation with oxidative status biomarkers and salicylic and jasmonic acids imbalances. Eur J Plant Pathol 163:203–221
Paciolla C, Ippolito MP, Logrieco AF et al (2008) A different trend of antioxidant defence responses makes tomato plants less susceptible to beauvericin than to T-2 mycotoxin phytotoxicity. Physiol Mol Plant Pathol 72:3–9
Paciolla C, Paradiso A, de Pinto MC (2016) Cellular redox homeostasis as central modulator in plant stress response. In: Gupta D, Palma J, Corpas F (eds) Redox State as a Central Regulator of Plant-Cell Stress Responses. Springer, Cham, pp 1–23
Paciolla C, Fortunato S, Dipierro N et al (2019) Vitamin C in plants: from functions to biofortification. Antioxidants (Basel) 8:519
Patel H, Ewels P, Peltzer A et al (2024) nf-core/rnaseq: nf-core/rnaseq v3.14.0 - Hassium Honey Badger (3.14.0). Zenodo. https://doi.org/10.5281/zenodo.10471647
Patro R, Duggal G, Love M et al (2017) Salmon: fast and bias-aware quantification of transcript expression using dual-phase inference. Nat Methods 14:417–419
Picot A, Atanasova-Pénichon V, Pons S et al (2013) Maize kernel antioxidants and their potential involvement in Fusarium ear rot resistance. J Agric Food Chem 61:3389–3395
Plett JM, Cvetkovska M, Makenson P et al (2009) *Arabidopsis* ethylene receptors have different roles in Fumonisin B1-induced cell death. Physiol Mol Plant Pathol 74:18–26
Poór P, Takacs Z, Bela K et al (2017) Prolonged dark period modulates the oxidative burst and enzymatic antioxidant systems in the leaves of salicylic acid-treated tomato. J Plant Physiol 213:216–226
Qin X, Zhang RX, Ge S et al (2017) Sphingosine kinase AtSPHK1 functions in fumonisin B1-triggered cell death in *Arabidopsis*. Plant Physiol Biochem 119:70–80
Renaud JB, Des Rochers N, Hoogstra S, Garnham CP, Sumarah MW (2021) Structure activity relationship for fumonisin phytotoxicity. Chem Res Toxicol 34:1604–1611
Sabetta W, Paradiso A, Paciolla C et al (2017) Chemistry, biosynthesis, and antioxidative function of glutathione in plants. In: Hossain M, Mostofa M, Diaz-Vivancos P, Burritt D, Fujita M, Tran LS (eds) glutathione in plant growth, development, and stress tolerance. Springer, Cham, pp 1–27
Santner A, Estelle M (2010) The ubiquitin-proteasome system regulates plant hormone signaling. Plant J 61:1029–1040
Schimittgen TD, Livak KJ (2008) Analyzing real-time PCR data by the comparative C(T) method. Nat Protocols 3:1101–1118
Shi L, Bielawski J, Mu J et al (2007) Involvement of sphingoid bases in mediating reactive oxygen intermediate production and programmed cell death in *Arabidopsis*. Cell Res 17:1030–1040
Singleton VL, Orthofer R, Lamuela-Raventos RM (1999) Analysis of total phenols and other oxidation substrates and antioxidants by means of Folin-Ciocalteu reagent. Meth Enzymol 299:152–178
Stone JM, Heard JE, Asai T et al (2000) Simulation of fungal-mediated cell death by fumonisin B1 and selection of fumonisin B1–resistant (fbr) *Arabidopsis* mutants. Plant Cell 12:1811–1822
Teow CC, Truong V, Mcfeeters RF et al (2007) Antioxidant activities, phenolic and β-carotene contents of sweet potato genotypes with varying flesh colours. Food Chem 103:829–838
Wang Y, Peng X, Xu W et al (2012) Transcript and protein profiling analysis of OTA-induced cell death reveals the regulation of the toxicity response process in *Arabidopsis thaliana*. J Exp Bot 63:2171–2187
Wang X, Wu Q, Wan D et al (2016) Fumonisins: oxidative stress-mediated toxicity and metabolism *in vivo* and *in vitro*. Arch Toxicol 90:81–101
Wu JX, Wu JL, Yin J et al (2015) Ethylene modulates sphingolipid synthesis in *Arabidopsis*. Front Plant Sci 6:1122
Xing F, Li Z, Sun A et al (2013) Reactive oxygen species promote chloroplast dysfunction and salicylic acid accumulation in fumonisin B1-induced cell death. FEBS Lett 587:2164–2172
Yanagawa D, Ishikawa T, Imai H (2017) Synthesis and degradation of long-chain base phosphates affect fumonisin B1-induced cell death in *Arabidopsis thaliana*. Int J Plant Res 130:571–585
Yates IE, Arnold JW, Hinton DM et al (2011) *Fusarium verticillioides* induction of maize seed rot and its control. Canad J Bot 81:422–428
Ye C, Zheng S, Jiang D et al (2021) Initiation and execution of programmed cell death and regulation of reactive oxygen species in plants. Int J Mol Sci 22:12942
Yekkour A, Tran D, Arbelet-Bonnin D et al (2015) Effect of *Fusarium* mycotoxin deoxynivalenol on *Nicotiana tabacum* cells: early events lead to programmed cell death. Plant Sci 238:148–157
Zeng LR, Vega-Sánchez ME, Zhu T et al (2006) Ubiquitination-mediated protein degradation and modification: an emerging theme in plant-microbe interactions. Cell Res 16:413–426
Zeng HY, Li CY, Yao N (2020) Fumonisin B1: a tool for exploring the multiple functions of sphingolipids in plants. Front Plant Sci 1:600458
Zhang J, Kirkham MB (1996) Enzymatic responses of the ascorbate-glutathione cycle to drought in sorghum and sunflower plants. Plant Sci 113:139–147
Zhang X, Wu Q, Cui S et al (2015) Hijacking of the jasmonate pathway by the mycotoxin fumonisin B1 (FB1) to initiate programmed cell

death in *Arabidopsis* is modulated by RGLG3 and RGLG4. J Exp Bot 66:2709–2721

Zhao Y, Wang J, Liu Y et al (2015) Classic myrosinase-dependent degradation of indole glucosinolate attenuates fumonisin B 1-induced programmed cell death in *Arabidopsis*. Plant J 81:920–933

Zhao Y, Liu Z, Wang L et al (2022) Fumonisin B1 as a tool to explore sphingolipid roles in *Arabidopsis* primary root development. Int J Mol Sci 23:12925